# Preparation and Crystalline Analysis of High-Grade Bamboo Dissolving Pulp for Cellulose Acetate

**Jianxin He,[1,2] Shizhong Cui,[2] Shan-yuan Wang[1]**

[1]*College of Textiles, Dong Hua University, Shanghai 201620, People's Republic of China*
[2]*College of Textiles, Zhongyuan University of Technology, Zhengzhou 450007, People's Republic of China*

Received 12 October 2006; accepted 6 February 2007
DOI 10.1002/app.27061
Published online 1 October 2007 in Wiley InterScience (www.interscience.wiley.com).

**ABSTRACT:** High grade bamboo dissolving pulp for cellulose acetate (named as acetate bamboo pulp) was prepared from bamboo Cizhu (*Dendrocalamus affinnis*) by oxygen-alkali pulping, xylanase and DMD (an intermediate product of the reaction of oxone with acetone) delignification treatments, and $H_2O_2$ bleaching. Its properties and structures were investigated by different analytical techniques, and compared with those of high grade hardwood dissolving pulp for cellulose acetate (named as acetate wood pulp), viscose bamboo pulp, and bamboo fiber for textile. Most of its properties are comparable with those of acetate wood pulp except ash contents and DCM (dichloromethane) extractive that are slightly high. Crystallinities and crystalline allomorphs of acetate bamboo pulp and the three samples were determined by FTIR spectroscopy, X-ray diffraction and solid state $^{13}C$ NMR spectroscopy, and the results obtained by the three methods were coincident. Bamboo cellulose crystalline allomorphs are classified as $I_\beta$-dominant type, and a higher lateral order index and a larger crystallite size for acetate bamboo pulp were found in spite of its crystallinity similar to acetate wood pulp. Different intermolecular hydrogen bond patterns are likely be responsible for the predominant crystalline fibrils in acetate bamboo pulp.  J Appl Polym Sci 107: 1029–1038, 2008

**Key words:** bamboo dissolving pulp; cellulose acetate; crystalline structure; $^{13}C$ NMR; FTIR

## INTRODUCTION

Cellulose acetate, being important in textile and cigarette industries, is prepared from high quality celluloses such as cotton linters and high-grade wood pulps with alpha cellulose content of more than 95%.[1] Cotton linters, the ideal material for cellulose acetate production, are limited to planting area and climate. High-grade wood pulps come from high quality hardwoods and softwoods of more than 20 years, which are restricted to fell, owing to environment protection policy.

Bamboo is a woody herbaceous plant, which consists of many vascular bundles and xylem.[2] A vascular bundle includes four sheaths of fibers, two vessels, and some sieve tubes. Xylem surrounds each vascular bundle. The sheath consists of many single fibers whose diameter is 10–20 nm each in average.[3,4] There are 1250 species of bamboos within 75 genera in the world, among which Asia accounts for about 1000 species, covering an area of over 180,000 km$^2$.[5]

*Correspondence to:* J. He (hejianxin771117@163.com).
Contract grant sponsor: Key Science and Technology Program of Henan Province; contract grant number: 052SYG26140.




Among natural fiber plants, bamboo is a kind of rapidly grown and early harvested vegetable with high adaptability, which is not like tree to suffer insect infestation. After grown 3 years, bamboo can be felled every year within several decades to 100 years. Unfortunately, bamboo is only employed in conventional applications such as furniture, construction, paper industry throughout the Asian region in spite of its superior properties like biodegradability, low cost, regeneration, and widespread utilization.[6] There are limited reports in the scientific literature concerning the use of bamboo pulp fiber, and a few researches focus on that bamboo pulp is used as reinforcing material of composite or employed in paper making.[3–7] Recently, bamboo pulp has been utilized in preparing viscose fiber in some Asia countries, but there is no report about bamboo material used in preparing cellulose acetate due to the higher requirements for the quality of pulp.

The aim of this study was to prepare high grade bamboo dissolving pulp for cellulose acetate from bamboo Cizhu. Cellulose I has two crystallization modifications $I_\alpha$ and $I_\beta$, assigned to the triclinic and monoclinic system, respectively, which depend on cellulose origin.[8] The contents of the two crystalline allomorphs in various origins have been investigated by many methods.[9] However, there is no report about the amount of two crystalline modifications in

**TABLE I**
**Bleaching Conditions**

| Stages | Pulp consistency (%) | Chemical charge | Temperature (°C) | Time (min) | pH |
|---|---|---|---|---|---|
| *X* | 10 | 0.5% DTPA, 0.04% xylanase | 70 | 90 | 6.5 |
| *P* | 10 | 5% $H_2O_2$, 2% NaOH 0.5% EDTA, 0.5% $MgSO_4$ | 70 | 120 | |
| *D* | 10 | oxone 8 g/L, acetone 6 g/L | 60 | 100 | 7.0–7.5 |
| *E* | 10 | 2% NaOH | 60 | 60 | |

bamboo cellulose. Thus relative $I_\alpha$ and $I_\beta$ content and crystalline structure in acetate bamboo pulp were also investigated by FTIR spectroscopy, X-ray diffraction, and solid state $^{13}C$ NMR spectroscopy, and compared with those of acetate wood pulp and other two bamboo celluloses: bamboo fiber and viscose bamboo pulp.

## EXPERIMENTAL

### Materials

The bamboo material chosen was Cizhu (*Dendrocalamus affinnis*) from Zhejiang province of China. Xylanase used in experiment was xylanase Pulpzyme HC provided by Novozyme, Denmark, with optimum activity at 70°C and pH 6.5. Oxone was from Dupont. Acetate wood pulp prepared by prehydrolyzed kraft pulping from Rayonier, viscose bamboo pulp prepared by prehydrolyzed kraft pulping from Shanghai pulp factory, and bamboo fiber for textile from Zhejiang bamboo fiber research center were used in experiments to investigate crystalline structure of acetate bamboo pulp. All other chemicals used were purchased from local company as analytical reagents and used without further purification.

### Cooking

Bamboo chips from the internodes of 2 × 1 $cm^2$ size were soaked in water about 8 h, and then were prehydrolyzed and cooked in autoclaves. In the prehydrolysis step bamboo chips and water with a ratio of 1 : 10 were charged, then 5% $H_2SO_4$ based on the dry weight of bamboo chips were added in, and the autoclave was heated to 100°C under a heating rate of 3°C/min and kept at 100°C for 200 min. The autoclave was then cooled to about 50°C and emptied, and the chips were washed with hot water. The yield was 79.8%.

Cooking step was then performed about 180 min with 13% NaOH, 0.05% anthraquinone (AQ), 1% Heteropoly Acid (HPA), 1% $MgCl_2$ at 0.8 MPa $O_2$-pressure, and the maximum cooking temperature of 160°C. The time at maximum temperature was about 40 min, and the liquor to bamboo ratio was 7 : 1. HPA can increase the selectivity of oxygen delignification and decrease the degradation of carbohydrate for its synergic action with oxygen to enable aromatic rings in lignin to be opened and decomposed into organics and carbon dioxide.[10] The black liquor was separated from the pulp by pressing in a nylon washing bag. The pulp in this bag was then thoroughly washed using a water shower. The total yield was determined as 37%.

### Bleaching

The pulp was bleached in polyethylene bag in water bath, using the XPDEP sequence, and here X, P, D, E indicated xylanase treatment stage, $H_2O_2$ bleaching stage, DMD treatment stage, and alkaline extraction stage, respectively. The conditions of bleaching are listed in Table I. The pulp was immersed in $NaH_2PO_4/Na_2HPO_4$ buffer solution of pH 6.5 for 60 min before treated by xylanase in X stage, and DTPA as metal ion chelator can decrease useless degradation of $H_2O_2$ in latter P stage. DMD, a reagent of delignification, is a intermediate product of the reaction of oxone ($2KHSO_5 \cdot KHSO_4 \cdot K_2SO_4$) with acetone, and the reaction equation is shown in Figure 1.[11,12] DMD having stronger electrophilic oxidation susceptibility can react with C=C, a dominate chromophoric group, in aliphatic and aromatic configurations in lignin by transferring active oxygen atoms (Fig. 2), thus improve the brightness of pulp.[11–13] The final yield of pulp after washed and dried was 13%.

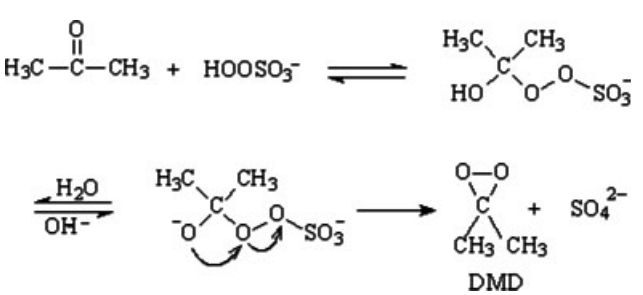


**Figure 1** Formation of DMD.

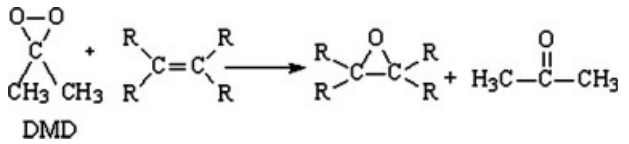


**Figure 2** Reaction of DMD with C=C in lignin.

### Chemical analysis

The degree of polymerizations (DP) of cellulose samples were determined from the intrinsic viscosities [η], which were measured using a Cannon-Fenske Routine Viscometer in a cupri-ethylene-diamine (CED) solution at 25°C according to TAPPI (Technical Association of the Pulp & Paper Industry, America) T206, by the formula of $DP^{0.905} = 0.75[\eta]/mL\ g^{-1}$. The contents of carbohydrate components such as cellulose, lignin, and pentose, solubility experiments, and ash contents were determined for raw material or cellulose samples using TAPPI standard methods. Brightness was measured according to ISO 3688/2470.

### Scanning electron microscopy

The samples were coated with gold film or embedded with epoxy resin in order to observe the surface morphology and the microstructure. The instrument was a JEOL JSM-5600LV electron microscopic with an accelerating voltage of 15 kV.

### FTIR spectroscopy

A mixture of 5.0-mg dried cellulose powders obtained from samples and 200 mg KBr were pressed into a disk for FTIR measurement in a Nicolet Nexus670 FTIR spectrometer. A total of 100 scans were taken for each sample with resolution of 2 $cm^{-1}$.

### X-ray diffractometry

X-ray diffraction was recorded at room temperature from 5° to 50° at a scanning speed of 0.02°/s with a Rigaku-D/Max-2550PC diffractometer using Ni-filtered Cu Kα radiation of wavelength 0.1542 nm. The operating voltage and current were 40 kV and 30 mA, respectively.

Crystallinities of celluloses in samples were calculated from diffraction intensity data using three different methods.[8,14] The first one assumes a two phase structure (crystalline-amorphous) and a line between the intensity minima to obtain an arbitrary background to diffraction trace, thus separating an arbitrary crystalline phase from an amorphous phase, the crystallinity $X_{cr}$ was calculated by:

$$X_{cr} = \frac{A_{cr}}{A_{cr} + A_{am}} \times 100\%$$

where $A_{cr}$ and $A_{am}$ are the integrated areas of the crystalline and amorphous phases, respectively.

In the second deconvolution method, the diffraction profile was fitted by Lorentzian function, ranging from 2θ 5° to 40°, to find the contribution of each individual peak relative to the 101, 10-1, 002, 040 crystallographic planes and the amorphous background. The maximum of amorphous peak was measured from the minimum of the diffraction profile between the 10-1 and 002 peaks. The crystallinity $X_d$ was calculated by:

$$X_d = \left[1 - \frac{S_a}{S_a + S_{cr}}\right] \times 100\%$$

where $S_a$ is the amorphous integrated area, and $S_{cr}$ is the sum of the integrated areas of the 101, 10-1, 002, 040 peaks.

The third approach was the empirical method proposed by Segal et al. for native cellulose:[14]

$$\mathrm{CrI} = \frac{I_{002} - I_{\mathrm{Amorph}}}{I_{002}} \times 100\%$$

where CrI is the crystallinity index, $I_{002}$ is the maximum intensity of the (002) lattice diffraction and $I_{\mathrm{Amorph}}$ is the diffraction intensity at 18° 2θ degrees.

The average size of crystallite was calculated from the Scherrer equation with the method based on the width of the diffraction patterns obtained in the X-ray reflected crystalline region. In this study, the crystallite sizes were determined by using the diffraction pattern obtained from the 002 (hkl) lattice planes of cellulose samples[15]:

$$D_{(\mathrm{hkl})} = \frac{k\lambda}{B_{(\mathrm{hkl})} \cos\theta}$$

where (hkl) is the lattice plane, $D$(hkl) is the size of crystallite, $k$ is the Scherrer constant (0.84), λ is the X-ray wavelength (0.154 nm), $B$(hkl) is the FWHM (full width half maximum) of the measured hkl reflection and 2θ is the corresponding Bragg angle (reflection angle).

### $^{13}$C-CP/MAS NMR

All the $^{13}$C-CP/MAS NMR measurements were performed with a Bruker AV400 NMR spectrometer operating at 75.5 MHz for carbons. The spinning speed was 5000 Hz, acquisition time 20 ms, contact time 1 ms and delay between pulses 3 s. All the cellulose samples were measured in never-dried (50 wt %).

**TABLE II**
**Chemical Composition of Bamboo Cizhu**

| Composition | Percentage based on dry material (%) |
|---|---|
| Cellulose | 51.09 |
| Lignin | 22.40 |
| Pentose | 21.60 |
| Ethanol-benzene extractive | 1.64 |
| 1% NaOH extractive | 22.26 |
| Hot-water extractive | 6.78 |
| Cold-water extractive | 2.42 |
| Ash | 1.53 |

## RESULTS AND DISCUSSION

### Chemical composition and physical properties of pulp

Chemical composition of Cizhu is shown in Table II. The result of chemical analysis shows that the cellulose content of Cizhu is similar to or higher than that of hardwood (42–51%), and higher than that of softwood (39–43%).[16,17] The lignin content of Cizhu is comparable with that of hardwood but lower than that of softwood (27–33%).[16,17] It is revealed that pentose, 1% NaOH extraction, hot and cold water extractions and ash content of Cizhu are higher than those of two kinds of woods, but the ethanol-benzene extraction of Cizhu is lower than that of wood (2–3%).[16,17] Overall the chemical analysis data shows that Cizhu is suitable for preparing high dissolving pulp, mainly because of its relatively low lignin, high cellulose and hemicelluloses content.

Table III summarizes composition, DP, and brightness of acetate bamboo pulp prepared as well as two pulp samples. It is shown that alpha cellulose content of acetate bamboo pulp is higher than that of viscose bamboo pulp, and comparable with that of acetate wood pulp sample, arriving at the demand for acetate dissolving pulp available commercially (>95%),[1] meanwhile, its DP is greater than that of viscose bamboo pulp, approaching that of acetate wood pulp (1000–1200). The visible insoluble substance in CED solution and the slower dissolution velocity were identified in the DP measurement of viscose bamboo pulp, while there was no the insoluble in acetate bamboo pulp. Mannose and xylose are representative neutral monosaccharides contained as hemicellulose in wood pulp, and derived from glucomannan and xylan, respectively. It was often reported for acetone solution of cellulose acetate that glucomannan acetate was a main cause of false viscosity and poor filterability, while xylan acetate was a main cause of haze, poor filterability, and coloring.[18–21] Acetate dissolving pulps available commercially contain mannose in a range between 0.3 and 1.5%, while 0.9 and 2.8% in xylose content.[1] As can be seen in Table III, the lower xylose content in acetate bamboo pulp compared with viscose bamboo pulp can be identified, and the content is in the controllable range in spite of the higher value compared with acetate wood pulp, considering there was no glucomannan in acetate bamboo pulp prepared because bamboo belongs herbaceous plants including no glucomannan. An obvious improvement of ISO brightness for acetate bamboo pulp can be found compared with viscose bamboo pulp and only 4.3% difference between it and acetate wood pulp indicates that the brightness of acetate bamboo pulp prepared has approached that of acetate dissolving pulp available commercially (90–96%).[1] The ash content and DCM extractive in acetate bamboo pulp, being higher greatly than that of acetate wood pulp, have not gone beyond the range of acetate dissolving pulp (ash $\leq$ 0.12, DCM extractive $\leq$ 0.08).[1]

### Morphological analysis

Bamboo pulp fiber is long cylindrical and uniform in size with distinct nodes [Figs. 3(a) and 4(a)], being different from wood pulp fiber which is flat without distinct nodes [Fig. 3(c)]. Figure 3(b,d) show the SEM images of acetate bamboo fiber and acetate wood fiber at magnification of 5000. It can be seen that there are full of grooves, splits, apertures, filaments and fibrils in two fiber surfaces, however bamboo fiber is straight with a smooth, sleek surface [Fig. 3(f)], showing no sign of formation of fibrils, and only a small quantity of cracks and fibrils in the surface of viscose bamboo pulp fiber [Fig. 3(e)]. This indicates that the same as acetate wood pulp, lignin, and hemicellulose in acetate bamboo pulp were removed using the pulping including xylanase and DMD treatment more fully than bamboo fiber and viscose bamboo pulp. This entirely removing of lignin and hemicellulose can also be seen from lengthwise section of acetate bamboo pulp in Figure 4(b), where distributing large numbers of apertures and cracks with uneven sizes besides inherent conduit.

**TABLE III**
**Comparison of Chemical Composition and Physical Properties of Acetate Bamboo Pulp with Acetate Wood Pulp and Viscose Bamboo Pulp**

| Parameters | Acetate bamboo pulp | Acetate wood pulp | Viscose bamboo pulp |
|---|---|---|---|
| Alpha cellulose (%) | 96.24 | 98.20 | 85.43 |
| DP | 1021 | 1134 | 512 |
| DCM extractive (%) | 0.08 | 0.013 | 0.22 |
| Xylose (%) | 3.9 | 1.3 | 6.8 |
| Mannose (%) | 0 | 0.3 | 0 |
| Brightness (%) | 88.4 | 92.7 | 75.5 |
| Ash (%) | 0.10 | 0.020 | 0.22 |
| Moisture (%) | 6.70 | 6.81 | 6.96 |

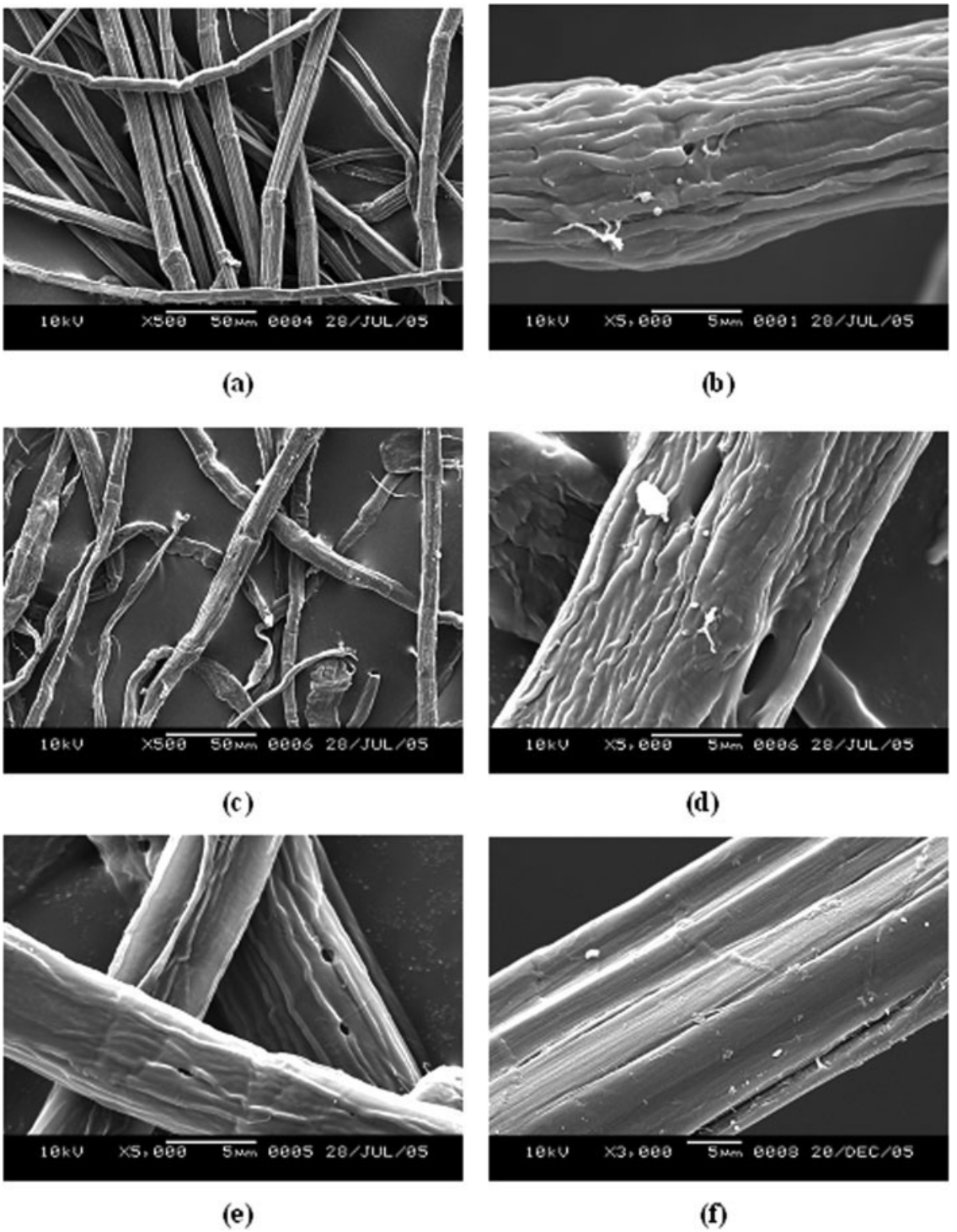


**Figure 3** SEM photographs of (a) pulp fiber surfaces of (b) acetate bamboo pulp, (c,d) acetate wood pulp, (e) viscose bamboo pulp, and (f) bamboo fiber.

## FTIR analysis

It can be seen from Figure 5 that FTIR spectra of acetate bamboo pulp and three samples show as the characteristic spectra of cellulose, and there are no vibration bands of aldehyde, ketonic, carboxyl groups from lignin and hemicellulose, but bamboo fiber has a faint band at 1739 $cm^{-1}$ attributed to the vibration of carboxyl group in hemicellulose.[22]

Figure 6 shows the second derivative FTIR spectra of acetate bamboo pulp and three samples in the range of OH group stretching. The band profiles in the 3400–3600 $cm^{-1}$ range[23,24] of intramolecular hydrogen bonds for three pulps are fairly similar,

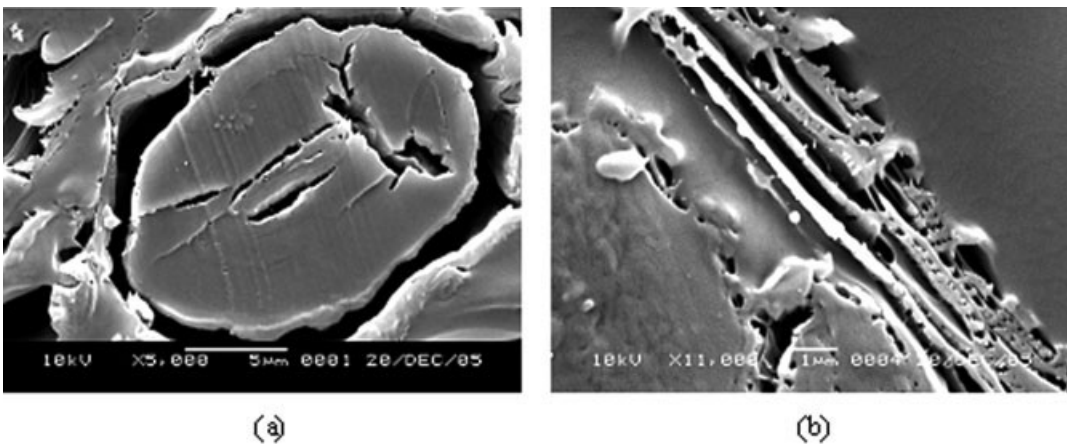


**Figure 4** SEM photographs of (a) cross section and (b) lengthwise section of acetate bamboo pulp.

and have a higher resolution, being different from bamboo fiber which has a lowest resolution in this range. The three bands around 3623, 3584, and 3570 $cm^{-1}$ are clearly resolved in the spectra of three pulps, while they are not distinguishable in the spectrum of bamboo fiber. Hence the lower crystallinities (see later) for two bamboo pulp compared with bamboo fiber most likely arise from the difference in the patterns of intramolecular hydrogen bond. The higher resolutions for acetate bamboo pulp and bamboo fiber in the band profiles in the 3200–3400 $cm^{-1}$ range[23,24] of intermolecular hydrogen bonds are observed compared with acetate wood pulp and viscose bamboo pulp. Thus predominant crystalline fibrils and biggish crystallite sizes in bamboo fiber and acetate bamboo pulp revealed by X-ray and $^{13}C$ NMR spectroscopy (see later) are probably related to the different intermolecular hydrogen bond pattern.

The second derivative FTIR spectra of four samples in the 900–500 $cm^{-1}$ fingerprint region show the similar profile with a very evident band around 712 $cm^{-1}$ and a inconspicuous band around 750 $cm^{-1}$ assigned to crystalline $I_\beta$ phase and $I_\alpha$ phase,[25] respectively (Fig. 7). Thus the crystalline allomorphs of three bamboo celluloses, the same as that of hardwood, were found as $I_\beta$-dominant type (monoclinic unit cell), which was not affected by extraction and pulping.

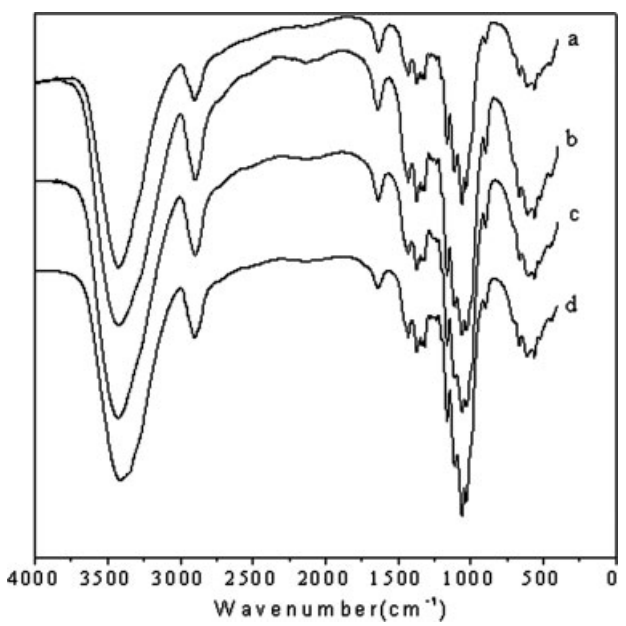


**Figure 5** FTIR spectra of (a) acetate bamboo pulp, (b) acetate wood pulp, (c) viscose bamboo pulp, and (d) bamboo fiber.

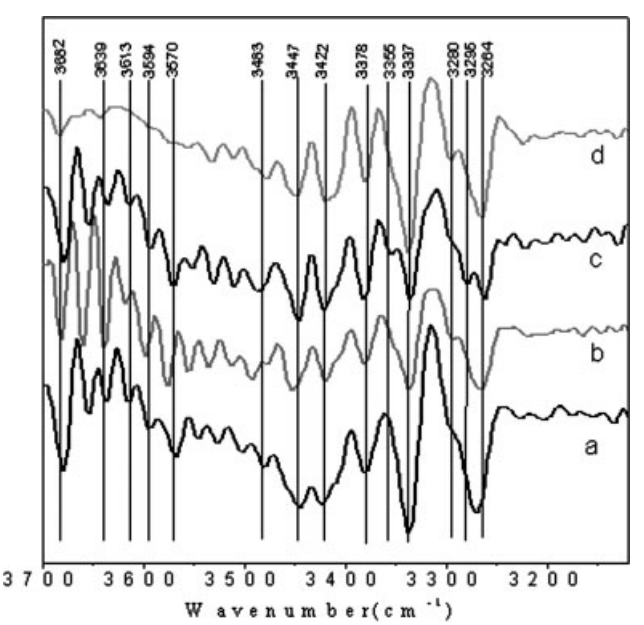


**Figure 6** Second derivative FTIR spectra (3700–3100 $cm^{-1}$) of (a) acetate bamboo pulp, (b) acetate wood pulp, (c) viscose bamboo pulp, and (d) bamboo fiber.

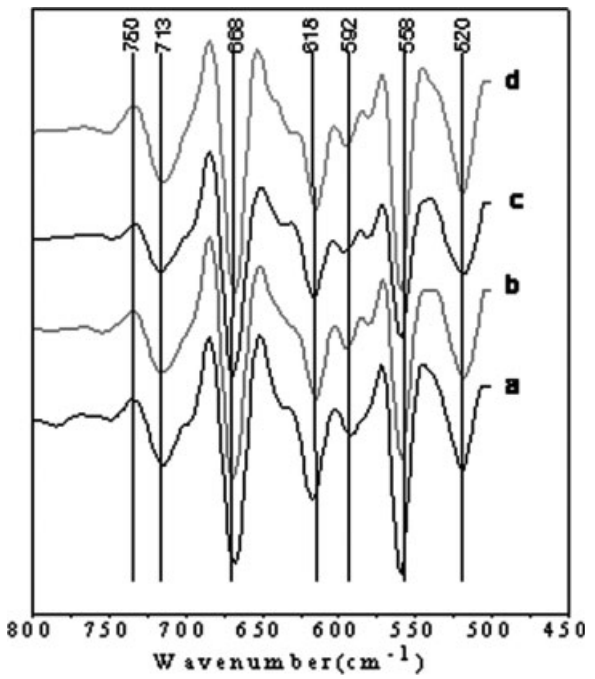


**Figure 7** Second derivative FTIR spectra (800–450 $cm^{-1}$) of (a) acetate bamboo pulp, (b) acetate wood pulp, (c) viscose bamboo pulp, and (d) bamboo fiber.

The ratio of the peak areas at 1370 and 670 $cm^{-1}$ (A1371/A665) proposed by Richter et al. was used to determine relative crystallinity index (CrI).[26] It was also used to study the conversion of cellulose I into cellulose II.[8,22,25,27] The lateral order index (LOI) of cellulose was evaluated using the intensity ratio of the bands at 1430 and 898 $cm^{-1}$, which is related to the proportion of cellulose I.[8,22,28] The two results are shown in Table IV. The highest CrI value in bamboo fiber and the lowest CrI value in viscose bamboo pulp were found, and the CrI value of acetate bamboo value was similar to that of acetate wood pulp, but the maximum LOI value in acetate bamboo pulp was also observed.

### X-ray diffraction analysis

The X-ray diffractograms of acetate bamboo pulp and three samples shown in Figure 8 are typical X-ray diffractograms of semi-crystalline cellulose I allomorph, and it is obvious that for bamboo fiber the diffractogram is well resolved and the crystallinity is uppermost, whereas for viscose bamboo pulp it is lowest (Table V). Being different from the results calculated by FTIR (Table IV), for acetate wood pulp the crystallinity calculated by the three different methods can be seen to be higher slightly than for acetate bamboo pulp. The cause for the difference is that the IR crystallinity index is correlated to the extent of the transition from cellulose I to cellulose II,[27] and a higher content of cellulose I in acetate bamboo pulp is likely to give rise to a higher CrI value. However compared with acetate wood pulp, acetate bamboo pulp possesses a larger crystallite size (Table V).

**TABLE IV**
**Crystallinity Indexes (CrI) and Lateral Order Indexes (LOI) in IR Spectra of Acetate Bamboo Pulp and Three Samples**

| | CrI | LOI |
|---|---|---|
| Samples | A1371/A665 | H1430/A898 |
| Acetate bamboo pulp | 6.417 | 1.994 |
| Acetate wood pulp | 6.243 | 1.403 |
| Viscose bamboo pulp | 5.771 | 1.168 |
| Bamboo fiber | 7.077 | 1.892 |

*Z*-discriminate function developed by Wada and coworkers was used to separate cellulose $I_\alpha$ and $I_\beta$ of native cellulose using *d*-spaces obtained from X-ray data.[9,25] The function used to discriminate is represented as: $Z = 1693d_1\text{-}902d_2\text{-}549$, where $Z > 0$ indicates the algal-bacterial ($I_\alpha$-rich) type and $Z < 0$ indicates the cotton-ramie ($I_\beta$-dominant) type. As can be seen in Table V, the crystalline allomorphs determined by *Z*-discriminate function for all bamboo celluloses and hardwood cellulose were found as $I_\beta$-dominant type without exception and the result is consistent with that of FTIR analysis.

### $^{13}$C-CP/MAS NMR analysis

The $^{13}$C-CP/MAS NMR spectra of acetate bamboo pulp and three samples are presented in Figure 9. It

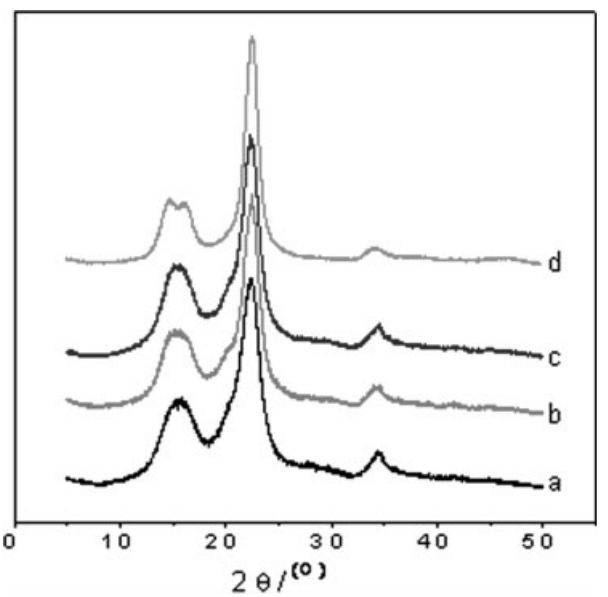


**Figure 8** X-ray diffractograms of (a) acetate bamboo pulp, (b) acetate wood pulp, (c) viscose bamboo pulp, and (d) bamboo fiber.

**TABLE V**
**Crystallinity, Crystallite Size, and Crystalline Allomorph of Acetate Bamboo Pulp and Three Samples**

| Samples | Crystallinity (%) | | | $D_{(002)}$ (nm) | *d*-spaces (nm) | | $Z$ | Allomorph |
|---|---|---|---|---|---|---|---|---|
| | $X_{cr}$ | CrI | $X_d$ | | $d_1$ | $d_2$ | | |
| Acetate bamboo pulp | 64.41 | 75.79 | 54.92 | 6.07 | 0.59824 | 0.54309 | −26.05 | $I_\beta$ |
| Acetate wood pulp | 65.72 | 78.61 | 58.27 | 5.98 | 0.59806 | 0.54067 | −24.17 | $I_\beta$ |
| Viscose bamboo pulp | 61.98 | 73.61 | 52.08 | 5.33 | 0.59832 | 0.54816 | −30.48 | $I_\beta$ |
| Bamboo fiber | 79.47 | 88.95 | 68.50 | 7.07 | 0.60636 | 0.54495 | −13.98 | $I_\beta$ |

was found that in contrast with acetate wood pulp and viscose bamboo pulp, acetate bamboo pulp and bamboo fiber showed two better resolved spectra, the expression of predominant crystalline fibrils, and it can be known that this difference most likely arises from the difference of intermolecular hydrogen bond pattern in four samples associating with the result of FTIR spectra analysis (Fig. 6). Table VI shows the $^{13}C$ peak assignments of different cellulose allomorphs.

The C1 resonance region at about 105 ppm in resolution enhancement spectra shown in Figure 10 splits to four signals, the inner two at 105.2 and 104.9 ppm being representative of cellulose $I_\alpha$ and paracrystalline proposed by wickholm et al.,[29] respectively; the outer two at 105.6 and 104.1 ppm assigned to cellulose $I_\beta$. The integration of obtained signals indicates the high $I_\beta$ contents (61–68%) for bamboo and hardwood, while the high $I_\alpha$ content for softwood documented by Newman.[30,31] This is coincident with the results obtained by FTIR and X-ray analysis. As is shown in Figure 10 and Table VI, the C4 signals of acetate bamboo pulp and three samples show the upfield wing associated with a less evident downfield shoulder, confirming the existence of $I_\alpha$ phase.

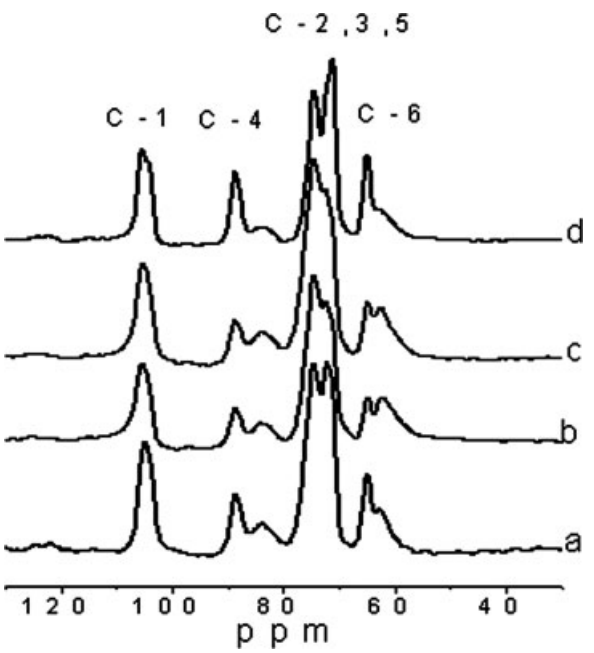


**Figure 9** $^{13}C$-CP/MAS NMR spectra of (a) acetate bamboo pulp, (b) acetate wood pulp, (c) viscose bamboo pulp, and (d) bamboo fiber.

As is shown in Figure 9, the two resonance regions associated with C6 and C4 include sharper resonances, assigned to the order region in crystal lattice, overlapping broader upfield wings, assigned to less order region that includes two categories of environment.[32] The first includes all chains located at the surfaces of cellulose microfibrils, which can be regarded as region of limited two-dimensional order. The second category of environment is the region within which the incoherence of order is not limited to two dimensions, and the chains are free to adopt a wider range of conformations than the ordering in a crystal lattice or their boundaries. Crystallinity index (CrI) was calculated from the percentage of the integrals of the C4 signals centered at 89 and 84 ppm presenting the crystalline and amorphous phase, shown in Table VII. Only 5% difference between acetate bamboo pulp and acetate wood pulp was found, but the fairly high LOI and crystallite size of acetate bamboo pulp resulted in good definition in the C2, 3, 5 resonance region. The sequence of CrI values for four cellulose samples calculated by $^{13}C$ NMR spectra is the same as that of the values calculated by FTIR analysis. As compared with the crystallinity values calculated by three methods of X-ray analysis, the crystallinity index calculated by $^{13}C$ NMR spectra shows the lowest relative values for all samples, more similar to the values applying the deconvolution method of X-ray analysis. The reason is that only material within the

**TABLE VI**
**Peak Assignment (ppm) of Cellulose Allomorphs in $^{13}C$-CP/MAS NMR Spectra**

| Allomorphs | Chemical shift | | |
|---|---|---|---|
| | C-1 | C-4 | C-6 |
| Cellulose II | 107.1 | 87.7 | 62.7, 61.2 |
| Cellulose $I_\beta$ | 105.6, 104.1 | 88.5 | 64.9 |
| Cellulose $I_\alpha$ | 105.2 | 89.5 | nd |
| Paracrystalline | 104.9 | 88.8 | 65.4 |

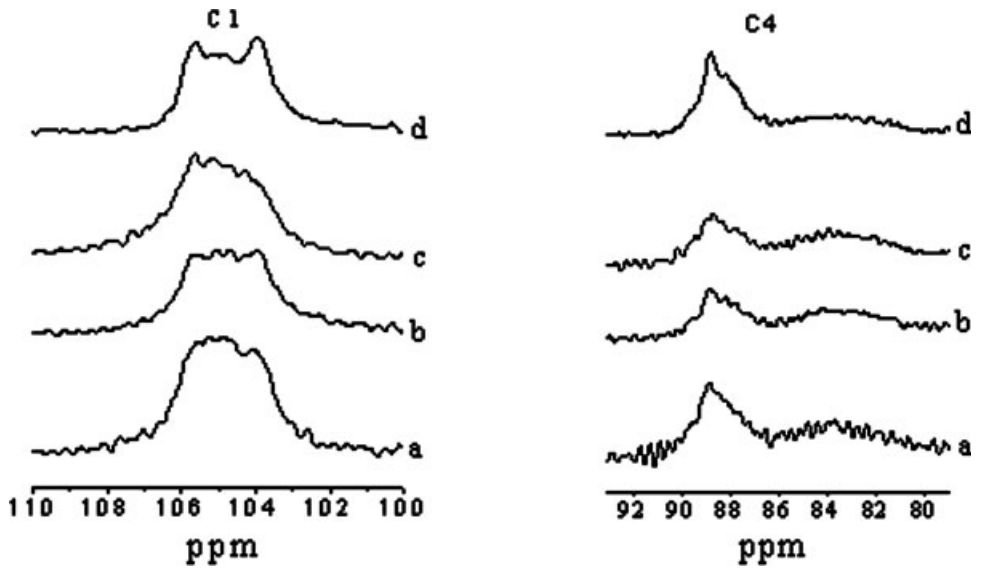


**Figure 10** The C1 and C4 regions in resolution enhancement $^{13}C$ NMR spectra of (a) acetate bamboo pulp, (b) acetate wood pulp, (c) viscose bamboo pulp, and (d) bamboo fiber.

crystalline domain appears as crystalline in $^{13}C$ NMR spectra, and the crystallinity calculated by NMR depends on crystallite size.[30]

Assuming that microfibrils contain only celluloses and the surface effect influences only the thickness of one chain, the lateral microfibril size can be determined from the signal intensities of the C-4 region of the spectrum, once a suitable model for the form of the microfibril cross-section is given. A simple model consists of a microfibril with a square cross-section with $(n + 2)$ chains per side and an infinite longitudinal size. The crystalline index evaluated from solid state NMR measurements, which is equivalent to the typical ratio of the chain number in crystalline core ($n^2$) to the total amount of cellulose, was calculated by the following formula.[33]

$$\mathrm{CrI} = \left(\frac{n}{n+2}\right)^2$$

The lateral microfibril size was calculated according to the formula $D = 0.58\ (n + 2)$, shown in Table VII, where the value 0.58 nm corresponds to the interchain distance.[34] It is revealed that the sequence of microfibril size values for acetate bamboo and three samples determined by $^{13}C$ NMR spectra was the same as that of the crystallite sizes calculated by X-ray analysis, but the values calculated by NMR are smaller than those obtained by X-ray diffraction except that of bamboo fiber. The difference observed between two methods can be a consequence of the hypotheses used in the calculation. The lateral size depends on crystallinity. Indeed, the higher the crystallinity of sample is, the larger the microfibrils lateral size is. In the hypotheses used, amorphous regions were assumed to be limited to the surface of microfibrils, which is probably true for the sample having high crystallinity such as bamboo fiber, but not for poorly crystalline samples such as those pulp samples, in which some amorphous and crystalline regions probably alternate along the microfibril. Secondly, the purity of microfibril is crucial for the size evaluation. The microfibril size correlates with the hemicellulose content, that is, a larger microfibril size correlates with a lower hemicellulose content.[33] Thus the actual microfibril size would be underestimated for sample with low alpha cellulose content such as viscose bamboo pulp. Moreover, a square crosssection was used in the calculations, whereas the facts are complicated and various shapes for crosssection of actual microfibril are possibly adopted. In contrast with X-ray analysis, $^{13}C$ NMR is more sensitive to short-range order.

**TABLE VII**
**Crystallinity Indexes (CrI), Contents of Crystalline Allomorphs, and Microfibril Sizes (*D*) in $^{13}C$ NMR Spectra of Acetate Bamboo Pulp and Three Samples**

| Samples | CrI (%) | $I_\alpha$ (%) | $I_\beta$ (%) | $D$ (nm) |
|---|---|---|---|---|
| Acetate bamboo pulp | 53.8 | 13.0 | 60.8 | 4.35 |
| Acetate wood pulp | 49.7 | 15.0 | 60.7 | 3.93 |
| Viscose bamboo pulp | 43.3 | 17.5 | 67.3 | 3.39 |
| Bamboo fiber | 73.6 | 14.3 | 68.3 | 7.86 |

## CONCLUSIONS

In this study, acetate bamboo pulp was prepared by oxygen-alkali pulping, xylanase and DMD treatments, and $H_2O_2$ bleaching. Its properties and struc-

tures were investigated by different analytical techniques, and compared with those of acetate wood pulp, viscose bamboo pulp and bamboo fiber. Chemical analysis showed the properties of acetate bamboo pulp came up to the requirements for cellulose acetate production, and SEM observation confirmed that lignin and hemicellulose in the surface and the inside were entirely removed. The FTIR results indicated that different intermolecular hydrogen bond patterns are likely be responsible for predominant crystalline fibrils in acetate bamboo pulp and bamboo fiber. $^{13}C$ NMR analysis showed cellulose $I_\beta$ allomorph contents of acetate bamboo pulp and three sample accounted for 61–68%, that is, the same as hardwood, bamboo cellulose was $I_\beta$-dominant type. This is coinciding with the results obtained by FTIR and X-ray analysis. A simple mode was used to calculate crystallite size of acetate bamboo pulp and three samples in $^{13}C$ NMR spectroscopy, and the sequence of the crystallite size values was coincident with that obtain by X-ray diffraction but the values obtained by $^{13}C$ NMR were smaller. This indicated that in contrast with X-ray analysis, $^{13}C$ NMR is more sensitive to short range order. The results obtained by three methods all showed that the crystallinity of acetate bamboo pulp was comparable with that of acetate wood pulp, but acetate bamboo pulp had the higher crystallite size and the higher LOI.

The authors thank Dr. Xu Peng for his help to paper writing.

## References


1. Shiro, S.; Hiroyuki, M. Macromol Symp 2004, 208, 37.
2. Thi, H. M. V.; Hannu, P.; Raimo, A. Ind Crops Prod 2004, 19, 49.
3. Tommy, Y. L.; Cui, H. Z.; Leung, H. C. Mater Lett 2004, 58, 2595.
4. Kazuya, O.; Toru, F.; Yuzo, Y. Compos A 2004, 35, 377.
5. Scurlocka, J. M. O.; Daytonb, D. C.; Hamesb, B. Biomass Bioenergy 2000, 19, 229.
6. Ray, A. K.; Das, S. K.; Mondal, S. J Mater Sci 2004, 39, 1055.
7. Okahisa, Y.; Yoshimura, T.; Imamura, Y. J Wood Sci 2005, 51, 542.
8. Focher, B.; Palma, M. T.; Canetti, M.; Torri, G.; Cosentino, C.; Gastaldi, G. Ind Crops Prod 2001, 13, 193.
9. Wada, M.; Okano, T.; Sugiyama, J. J Wood Sci 2001, 47, 124.
10. Evtuguin, D. V.; Neo, C. P. Pulp Paper Sci 1998, 24, 133.
11. Lee, C. L.; Hunt, K.; Murray, R. W. J Pulp Paper Sci 1994, 20, 125.
12. Hunt, K.; Lee, C. L. J Pulp Paper Sci 1995, 21, 263.
13. Hunt, K.; Lee, C. L.; Bourbonnais, R.; Paice, M. G. J Pulp Paper Sci 1998, 24, 55.
14. Segal, L.; Creely, L.; Martin, A. E.; Conrad, C. M. Textile Res J 1959, 29, 786.
15. Ahtee, M.; Hattula, T.; Mangs, J.; Paakkari, T. Paperi Ja Puu 1983, 8, 475.
16. Li, S. H.; Zeng, Q. Y.; Xiao, Y. L.; Fu, S. Y.; Zhou, B. L. Mater Sci Eng C 1995, 3, 125.
17. Timell, T. E. Wood Sci Technol 1967, 1, 45.
18. Neal, J. L. J Appl Polym Sci 1965, 9, 947.
19. Steinmann, H. W.; White, B. B. Tappi 1954, 37, 25.
20. Watson, J. K.; Henderson, D. R. Tappi 1957, 40, 686.
21. Conca, R. J.; Hamilton, J. K.; Kircher, H. W. Tappi 1963, 46, 644.
22. Ouajai, S.; Shanks, R. A. Polym Degrad Stabil 2005, 89, 327.
23. Fengel, D. Holzforschung 1992, 46, 283.
24. Focher, B.; Naggi, A.; Torri, G.; Cosani, A.; Terbojevich, M. Carbohydr Polym 1992, 17, 97.
25. Hinterstoisser, B.; Salmen, L. Cellulose 1999, 6, 251.
26. Ritcher, U.; Krause, T.; Schempp, W. Angew Macromol Chem 1991, 1851186, 155.
27. Akerholm, M.; Hinterstoisser, B.; Salmen, L. Carbohydr Res 2004, 339, 569.
28. Oh, S. Y.; Yoo, D. I.; Shin, Y.; Kim, H. C. Carbohydr Res 2005, 340, 2376.
29. Wickholm, K.; Larsson, P. T.; Iversen, T. Carbohydr Res 1998, 312, 123.
30. Maunu, S.; Liitia, T.; Kauliomaki, S.; Sundquist, J. Cellulose 2000, 7, 147.
31. Newman, R. H. J Wood Chem Technol 1994, 14, 451.
32. Atalla, R. H.; VanderHart, D. L. Solid State Nucl Magn 1999, 15, 1.
33. Heux, L.; Dinand, E.; Vignon, M. R. Carbohydr Polym 1999, 40, 115.
34. Rondeau-Mouro, C.; Bouchet, B.; Pontoirea, B.; Robert, P. Carbohydr Polym 2003, 53, 241.